SUPPORTING INFORMATION

Loop-Contraction Mutagenesis of Type 1 Copper Sites

Sachiko Yanagisawa and Christopher Dennison*

School of Natural Sciences, Bedson Building, University of Newcastle upon Tyne, Newcastle upon Tyne, NE1 7RU, U. K.

Table S1. Wavelengths (nm) of the LMCT and LF Transitions in the UV/Vis Spectra of Co(II)-Substituted Loop Variants and the Corresponding WT Proteins.

Ami[a]	Paz[b]	PazAmi	Pc[c]	PcAmi	Az[d]	AzAmi	Assignment
337	335	336	334	340	330	337	LMCT
388	390 (sh)[e]	398	385	391	375	385	LMCT
~436	440 (sh)			442 (sh)	405 (sh)		[f]
509	505	507	506	508	522	504	LF
~645	640 (sh)	641	653	640	638	640	LF
689	673	685	674	690	645 (sh)	670	LF

[a] *P. versutus* amicyanin at pH 8.2 and 25 ^{o}C. [b] *A. cycloclastes* pseudoazurin at pH 8.0 and 25 ^{o}C. [c] Spinach plastocyanin at pH 8.0 and 25 ^{o}C. [d] *P. aeruginosa* azurin at pH 8.0 and 25 ^{o}C. [e] Shoulder. [f] Not assigned.

Table S2. Hyperfine Shifted Resonances in the ^{1}H NMR Spectrum of Cu(II) PcAmi and their Diamagnetic Counterparts in the Cu(I) protein[a]

Resonance	δ_{obs} (ppm) in Cu(II) PcAmi	δ_{obs} (ppm) in Cu(I) PcAmi	Assignment
a	48.0	7.32	His87 $C^{\delta 2}H$
b	42.5	7.69	His37 $C^{\delta 2}H$
c	~33	7.80	His87 $C^{\varepsilon 1}H$
d	~29	7.17	His37 $C^{\varepsilon 1}H$
e	29.2[b]		His37 $N^{\varepsilon 2}H$
f	17.4	2.02	Met90 $C^{\gamma 2}H$
g	14.2	4.12	Asn38 $C^{\alpha}H$
h	10.5	3.07	Met90 $C^{\gamma 1}H$
j	-7.6	5.23	Cys84 $C^{\alpha}H$

[a] Data recorded at 40 ^{o}C in 37 mM phosphate buffer in 99.9 % D_2O at pH* 7.5. [b] Measured in 37 mM phosphate (90 % H_2O / 10 % D_2O) at pH 7.5 and 40 ^{o}C.

Table S3. Hyperfine-shifted resonances in the ^{1}H NMR spectrum of Co(II) PazAmi[a]

Resonance	δ_{obs} (ppm)	$\Delta\upsilon_{½}$ (Hz)	Assignment
a	338	2200	Cys78 $C^{\beta}H$
b	306	1700	Cys78 $C^{\beta}H$
c	285	450	Met84 $C^{\gamma}H$
d	~150	~2000	His40/81 $C^{\varepsilon 1}H$
e	99.8	650	Met84 $C^{\varepsilon}H_3$
f	95.0	750	Met84 $C^{\gamma}H$
g	63.1	170	His40 $N^{\varepsilon 2}H$
h	~63	~1200	His40/81 $C^{\varepsilon 1}H$
i	49.2	100	His40/81 $C^{\delta 2}H$
j	47.5	140	His40/81 $C^{\delta 2}H$

[a] Data recorded (25 ^{o}C) at 300 MHz in 10 mM phosphate at pH 8.1. Included are the observed chemical shifts (δ_{obs}), the peak widths ($\Delta\upsilon_{½}$) and the assignments that have been made. The assignment of this spectrum is straightforward from a comparison to the data for the WT protein (see Table S6). A strong NOE is observed between signals c and e (data not shown) confirming that these peaks arise from the geminal $C^{\gamma}H$ protons of the axial Met84 ligand. The intensity and isotropic shift of signal f identifies it as the $C^{\varepsilon}H_3$ of the same ligand. The large hyperfine shifts, line-widths and small T_1 values (< 1 ms) of signals a and b confirm that they arise from the Cys78 ligand $C^{\beta}H$ protons. The exchangeable signal g is readily assigned to the $N^{\varepsilon 2}H$ proton of the buried His40 ligand. The corresponding resonance of the exposed His81 ligand is only observed at low pH in Co(II) Paz and the instability of Co(II) PazAmi under these conditions prevents its detection.

Table S4. Hyperfine-shifted resonances in the ^{1}H NMR spectrum of Co(II) PcAmi[a]

Resonance	δ_{obs} (ppm)	$\Delta\upsilon_{½}$ (Hz)	Assignment
a	327	1800	Cys84 $C^{\beta}H$
b	316	1500	Cys84 $C^{\beta}H$
c	239	1000	Met90 $C^{\gamma}H$
d	~129	~2000	His37/87 $C^{\varepsilon 1}H$
e	91.9	nd[b]	Met90 $C^{\varepsilon}H_3$
f	90.8[c]	nd[b]	Met90 $C^{\gamma}H$
g	72.4	nd	His87 $N^{\varepsilon 2}H$
h	~65	~1600	His37/87 $C^{\varepsilon 1}H$
i	60.8	170	His37 $N^{\varepsilon 2}H$
j	51.9	70	His37 $C^{\delta 2}H$
k	45.8	120	His87 $C^{\delta 2}H$

[a] Data recorded (25 ^{o}C) at 300 MHz in 10 mM phosphate at pH 8.1. Included are the observed chemical shifts (δ_{obs}), the peak widths ($\Delta\upsilon_{½}$) and the assignments that have been made. Irradiation of peak c gives rise to a strong NOE to signal f (see Figure S7B) which overlaps with signal e (this composite signal has an intensity equivalent to four protons). Thus one of the $C^{\gamma}H$ signals of the axial Met90 overlaps with the $C^{\varepsilon}H_3$ resonance from this ligand. The characteristic properties of signals a and b identify them as the $C^{\beta}H$ protons of the Cys84 ligand. The exchangeable signal g, which is hardly observed at pH 8.1 is assigned to the exposed His87 ligand. The exchangeable signal i has a much greater intensity at pH 8.1 and is thus assigned to the buried His37 ligand. An NOE is observed between this peak and the relatively sharp resonance j (see Figure S7C) which identifies the latter as the $C^{\delta 2}H$ resonance from this His ligand. [b] Not determined due to spectral overlap. [c] Position determined from a 1D NOE difference experiment in which signal e was irradiated.

Table S5. Hyperfine-shifted resonances in the ^{1}H NMR spectrum of Co(II) AzAmi[a]

Resonance	δ_{obs} (ppm)	$\Delta\upsilon_{½}$ (Hz)	Assignment
a	346 (325)[b]	1800	Cys112 $C^{\beta}H$
b	254 (241)	1500	Cys112 $C^{\beta}H$
c	89.0 (84)	2900	His46/115 $C^{\varepsilon 1}H$
d	74.0 (70.1)	220	His46 $N^{\varepsilon 2}H$
e	70.7[c]	650	His115 $N^{\varepsilon 2}H$
f	49.7 (45.8)	200	Gly45 $C^{\alpha}H$
g	47.8 (45.3)	nd[d]	His46 $C^{\delta 2}H$
h	46.9 (44.7)	nd[d]	His115 $C^{\delta 2}H$
i	27.3 (26.1)	220	Met118 $C^{\gamma}H$
j	-13.2 (-12.3)[e]	120[e]	Met118 $C^{\beta}H$
k	-14.7 (-13.0)[e]	220[e]	Met118 $C^{\gamma}H$
l	-18.0 (-16.4)	200	Met118 $C^{\beta}H$
m	-27.7 (-25.0)	250	Gly45 $C^{\alpha}H$

[a] Data recorded (25 ^{o}C) at 300 MHz in 10 mM phosphate at pH 8.1. Included are the observed chemical shifts (δ_{obs}), the peak widths ($\Delta\upsilon_{½}$) and the assignments that have been made. The observed NOEs between signals a and b (data not shown) confirm that they belong to the geminal $C^{\beta}H$ protons of the Cys112 ligand. Irradiation of peaks a and b gives rise to NOEs to peaks j and l (see Figure S8B and C) which belong to a geminal pair of protons as a strong NOE is observed between them (see Figure S8D). In the structure of Cu(II) Az[23,24] and Ami[25] the coordinated Cys $C^{\beta}H$ protons point directly at the $C^{\beta}H$ protons of the axial Met ligand and thus signals j and l are assigned to the $C^{\beta}H$ protons of Met118. The irradiation of peak i gives rise to a strong NOE to signal k and a weaker NOE to j (see Figure S8E). The intense NOE between peaks i and k identifies them as a geminal pair of protons and the connection to j leads to their assignment as the Met118 $C^{\gamma}H$ protons. Signals f and m exhibit strong NOEs to each other

(see Figures S8F and G) and thus can be assigned to the $C^{\alpha}H$ protons of Gly45. This latter assignment is supported by the pattern of NOEs observed from signal m, which is remarkably similar to that observed when the $C^{\alpha 2}H$ resonance of Gly45 is irradiated in experiments on Co(II) Az.[45] Furthermore, the positive and negative δ_{obs} values for these two signals is analogous to what is observed for Co(II) Az and is completely consistent with the orientation of the magnetic susceptibility tensor.[46] Two exchangeable signals (peaks d and e) exhibiting sizable isotropic shifts are observed in the spectrum of Co(II) AzAmi in 90 % H_2O / 10 % D_2O at pH 8.1 and 5 ^{o}C (data not shown). One of these (signal e) is very weak and the other (peak d) has an intensity equivalent to one proton. Thus peak d can be assigned to the buried His46 $N^{\varepsilon 2}H$ proton whilst peak e arises from the exposed His115. Irradiation of peak d gives rise to an NOE to resonance g which can be assigned to the $C^{\delta 2}H$ of His46. [b] The values in parenthesis are those measured at 40 ^{o}C (pH 8.1). [c] Only observed at 5 ^{o}C at pH 8.1. [d] Not determined due to spectral overlap. [e] Position determined from a 1D NOE difference experiment.

Table S6. The observed hyperfine shifts (δ_{obs})[a] in the ^{1}H NMR spectrum of Co(II) loop variants compared with the δ_{obs} values for the corresponding resonances in the spectra of the WT Co(II) cupredoxins

Ligand[b]	Proton	Co(II) Ami[c] δ_{obs} (ppm)	Co(II) Paz[d] δ_{obs} (ppm)	Co(II) PazAmi[e] δ_{obs} (ppm)	Co(II) Pc[f] δ_{obs} (ppm)	Co(II) PcAmi[g] δ_{obs} (ppm)	Co(II) Az[h] δ_{obs} (ppm)	Co(II) AzAmi[i] δ_{obs} (ppm)
His	$H^{\delta 2}$	52.6	53.1	49.2/47.5	55.8	51.9	50.6	47.8
	$H^{\varepsilon 1}$	118/38	146/57	150/63	133	129/65	97	89
	$H^{\varepsilon 2}$	62.3	61.9	63.1	63.2	60.8	74.9	74.0
Cys	$H^{\beta 1}$	285	315/267	338/306	299	327	232	254
	$H^{\beta 2}$	285	315/267	338/306	275	316	285	346
His	$H^{\delta 2}$	51.0	43.6	49.2/47.5	43.8	45.8	56.4	46.9
	$H^{\varepsilon 1}$	118/38	146/57	150/63	60	129/65	75	89
	$H^{\varepsilon 2}$	74	71.4	-	75.3	72.4	65.8	70.7
Met	$H^{\beta 1}$	-18.6	-31.2	-	-18.4	-	-18.9	-18.0/-13.2
	$H^{\beta 2}$	-16.1	-	-	-27.5	-	-18.5	-18.0/-13.2
	$H^{\gamma 1}$	132.5	105.8	95	254	239	45.3	27.3
	$H^{\gamma 2}$	10.0	271.3	285	87.8	90.8	-19.1	-14.7
	$C^{\varepsilon}H_3$	74.5	90.2	99.8	80.4	91.9	-7.3	-
Gly	$H^{\alpha 1}$	-	-	-	-	-	47.8	49.7
	$H^{\alpha 2}$	-	-	-	-	-	-29.4	-27.7

[a] The interpretation of the δ_{obs} values of the isotropically shifted resonances in the paramagnetic NMR spectrum of a Co(II) cupredoxin is less straightforward than for the copper protein due to the greater magnetic anisotropy, and thus more significant δ_{pc} contributions [see footnote a of Table 2]. To calculate the δ_{pc} contributions to the isotropic shifts requires that the orientation and components of the magnetic susceptibility (χ) tensor be known. In the case of Co(II) azurin these have been determined and generate large negative δ_{pc} values for protons orientated towards the axial positions whilst those in the equatorial N_2S plane experience smaller positive δ_{pc} contributions to δ_{obs}.[46] It is assumed that the orientation and

components of the χ-tensor are similar in the various Co(II) cupredoxins and that the loop contractions do not have a significant influence on these. Therefore δ_{obs} values can be compared to provide information about the influence of the mutations on the spin density distribution at the active site. [b] From top to bottom: His54, Cys93, His96 and Met99 for Ami; His40, Cys78, His81 and Met86 for Paz; His40, Cys78, His81 and Met84 for PazAmi; His37, Cys84, His87 and Met92 for Pc; His37, Cys84, His87 and Met90 for PcAmi; His46, Cys112, His117, Met121 and Gly45 for Az; His46, Cys112, His115, Met118 and Gly45 for AzAmi. [c] Ami from *P. versutus* at 40 ^{o}C and pH 8.0 (the His96 $N^{\varepsilon 2}H$ resonance was observed at 22 ^{o}C and pH 5.0).[32] [d] Paz from *A. cycloclastes* at 40 ^{o}C and pH 8.0.[47] [e] This study at 25 ^{o}C and pH 8.1. [f] Spinach Pc at 30 ^{o}C and pH 7.8 (5 ^{o}C and pH 7.0 in the case of the His87 $N^{\varepsilon 2}H$ resonance).[34] [g] This study at 25 ^{o}C and pH 8.1. [h] Az from *P. aeruginosa* at pH 4.5 and 37 ^{o}C.[46,48] [i] This study at 25 ^{o}C and pH 8.1.

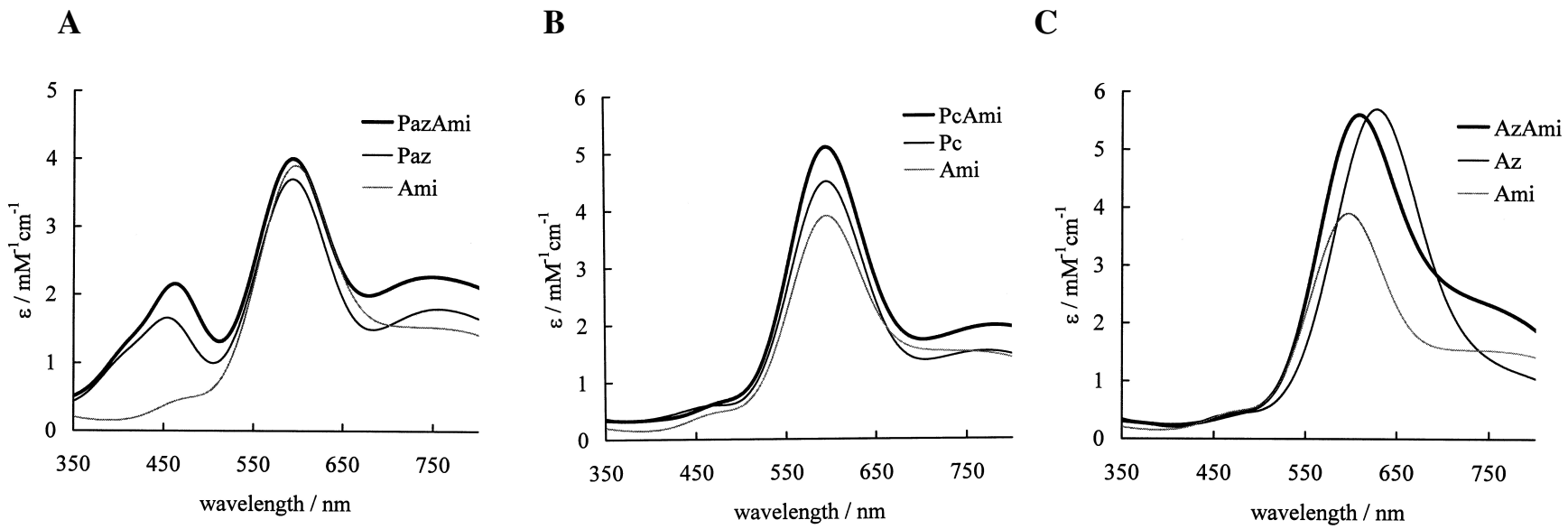

Figure S1. UV/Vis spectra of the Cu(II) proteins at 25 ^{o}C in 10 mM phosphate pH 8.0; (A) Paz, PazAmi and Ami, (B) Pc, PcAmi and Ami and (C) Az, AzAmi and Ami.

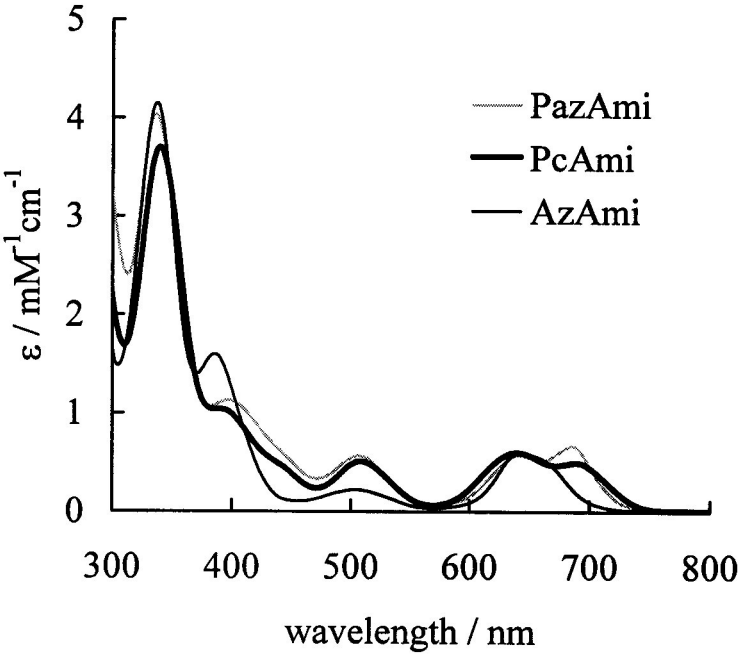

Figure S2. UV/Vis spectra (25 °C) of the Co(II) loop variants in 10 mM phosphate pH 8.0.

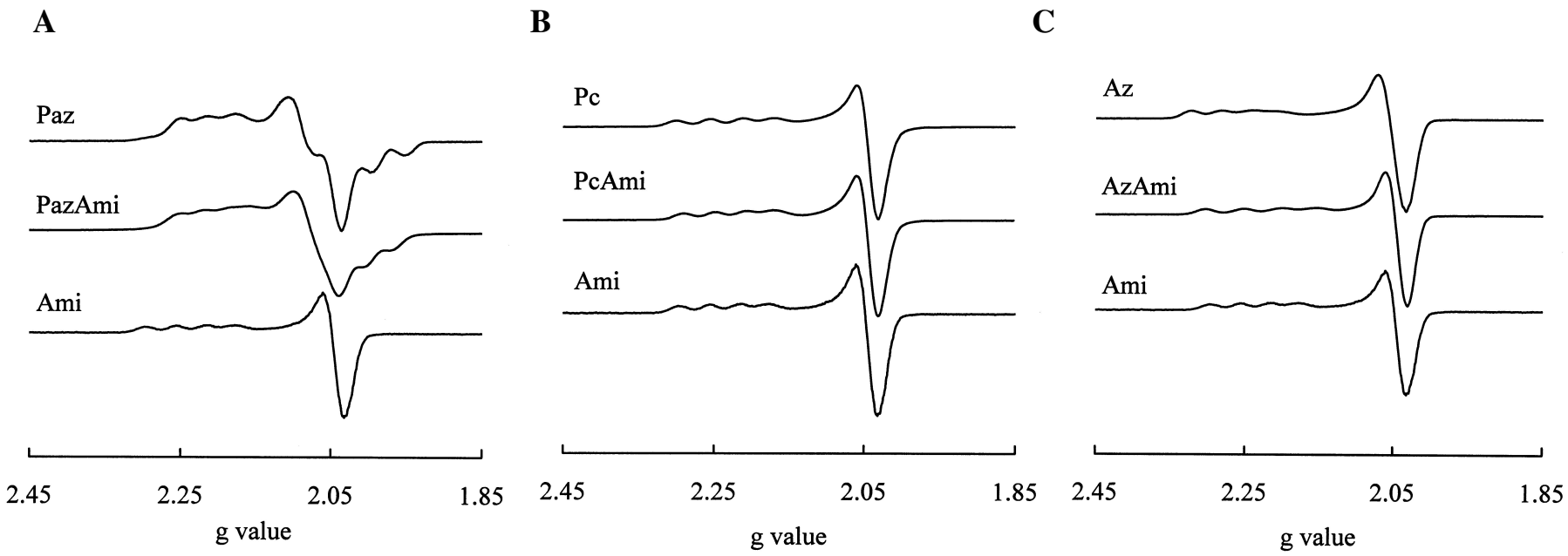

Figure S3. EPR spectra of the Cu(II) proteins at -196 ^{o}C in 25 mM Hepes pH 7.6 (40 % glycerol); (A) Paz, PazAmi and Ami, (B) Pc, PcAmi and Ami and (C) Az, AzAmi and Ami.

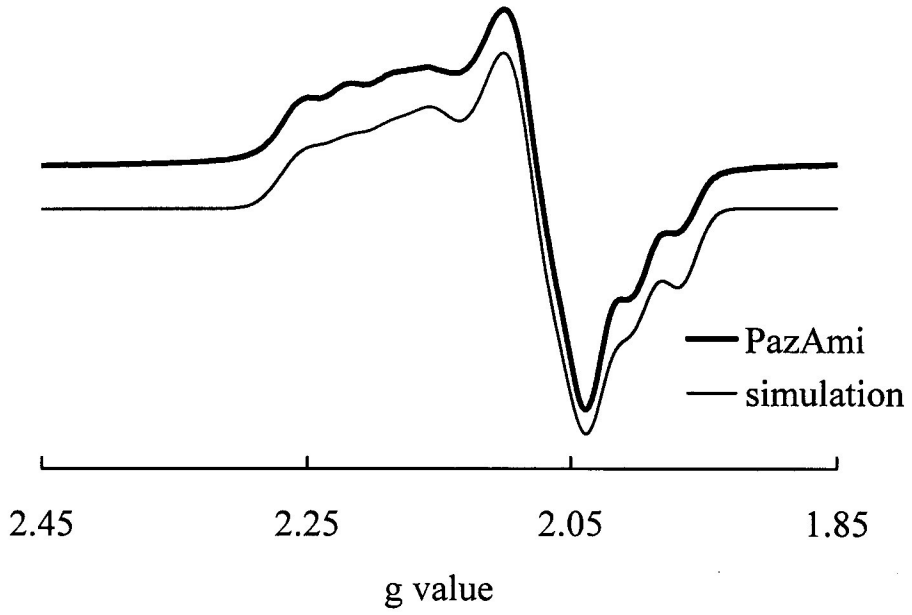

Figure S4A. EPR spectrum of PazAmi at -196 °C in 25 mM Hepes pH 7.6 (plus 40 % glycerol). Also shown is the simulated spectrum obtained using SimFonia (Bruker).

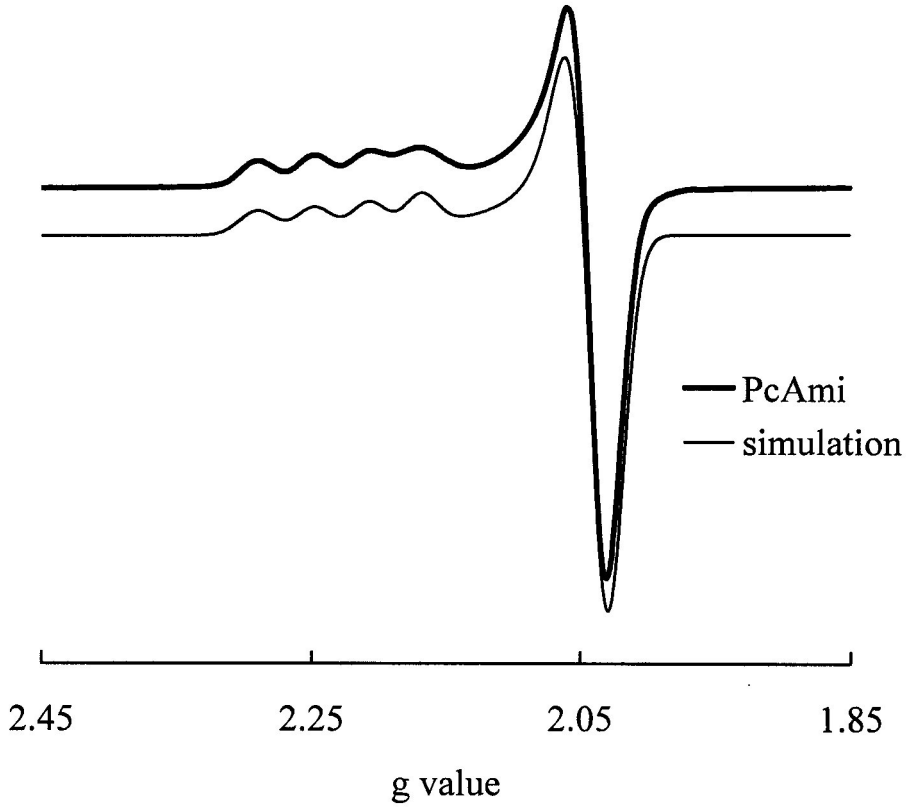

Figure S4B. EPR spectrum of PcAmi at -196 °C in 25 mM Hepes pH 7.6 (plus 40 % glycerol). Also shown is the simulated spectrum obtained using SimFonia (Bruker).

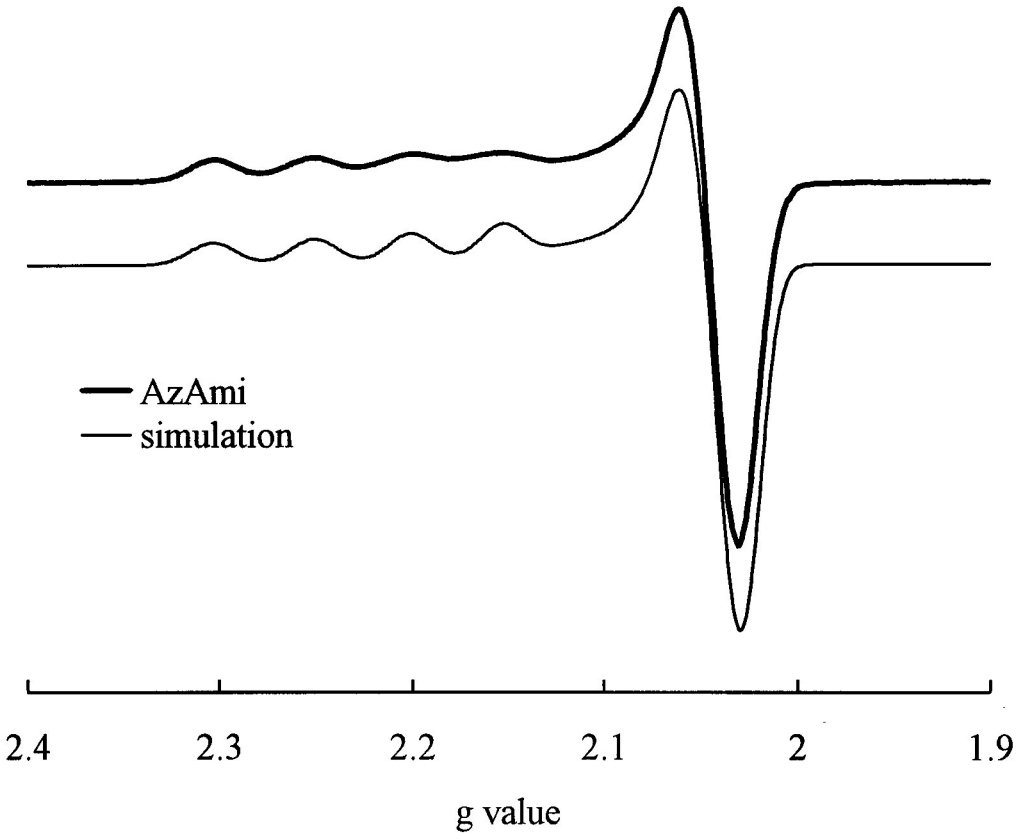

Figure S4C. EPR spectrum of AzAmi at -196 °C in 25 mM Hepes pH 7.6 (plus 40 % glycerol). Also shown is the simulated spectrum obtained using SimFonia (Bruker).

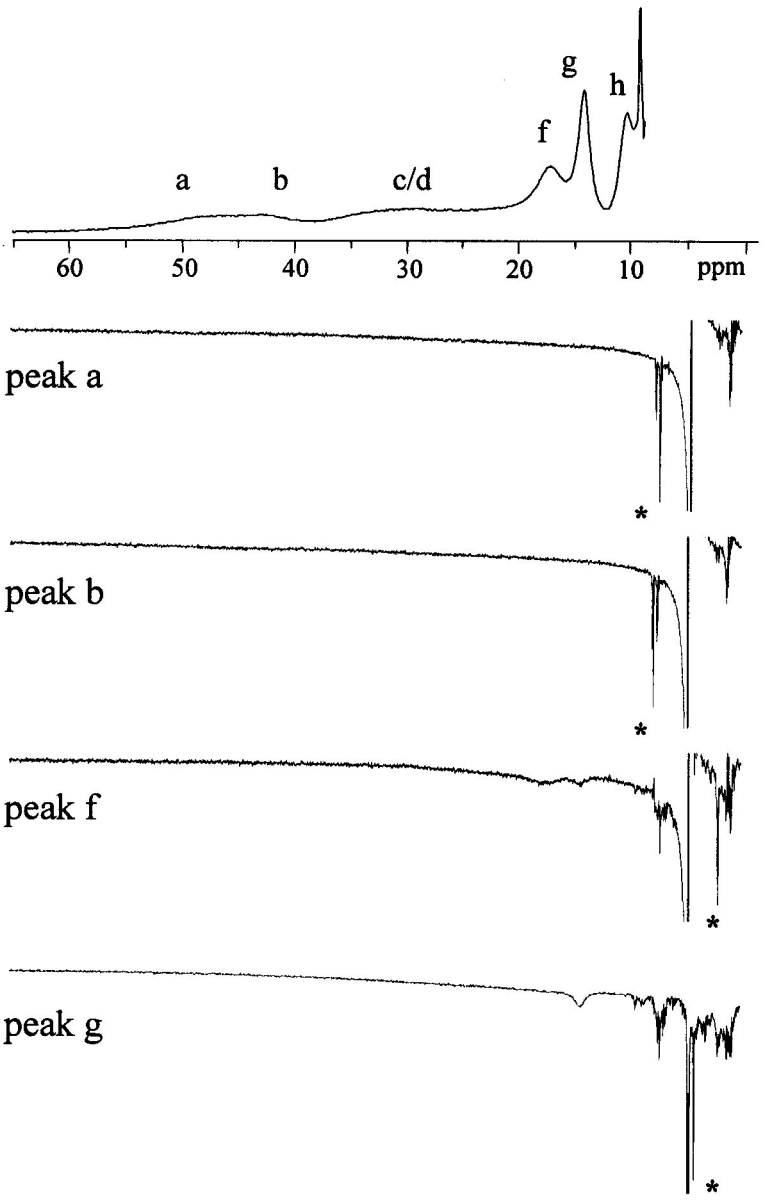

Figure S5. ^{1}H NMR saturation transfer difference spectra (500 MHz) of a mixture of Cu(I) (1.6 mM) and Cu(II) (1.6 mM) PcAmi in 37 mM phosphate (99.9 % D_2O) at pH* 7.5 (40 °C). The top spectrum is that of Cu(II) PcAmi and those below are the saturation transfer difference spectra in which the peaks indicated were irradiated. The observed saturation transfer peaks in the Cu(I) protein are shown by an asterisk.

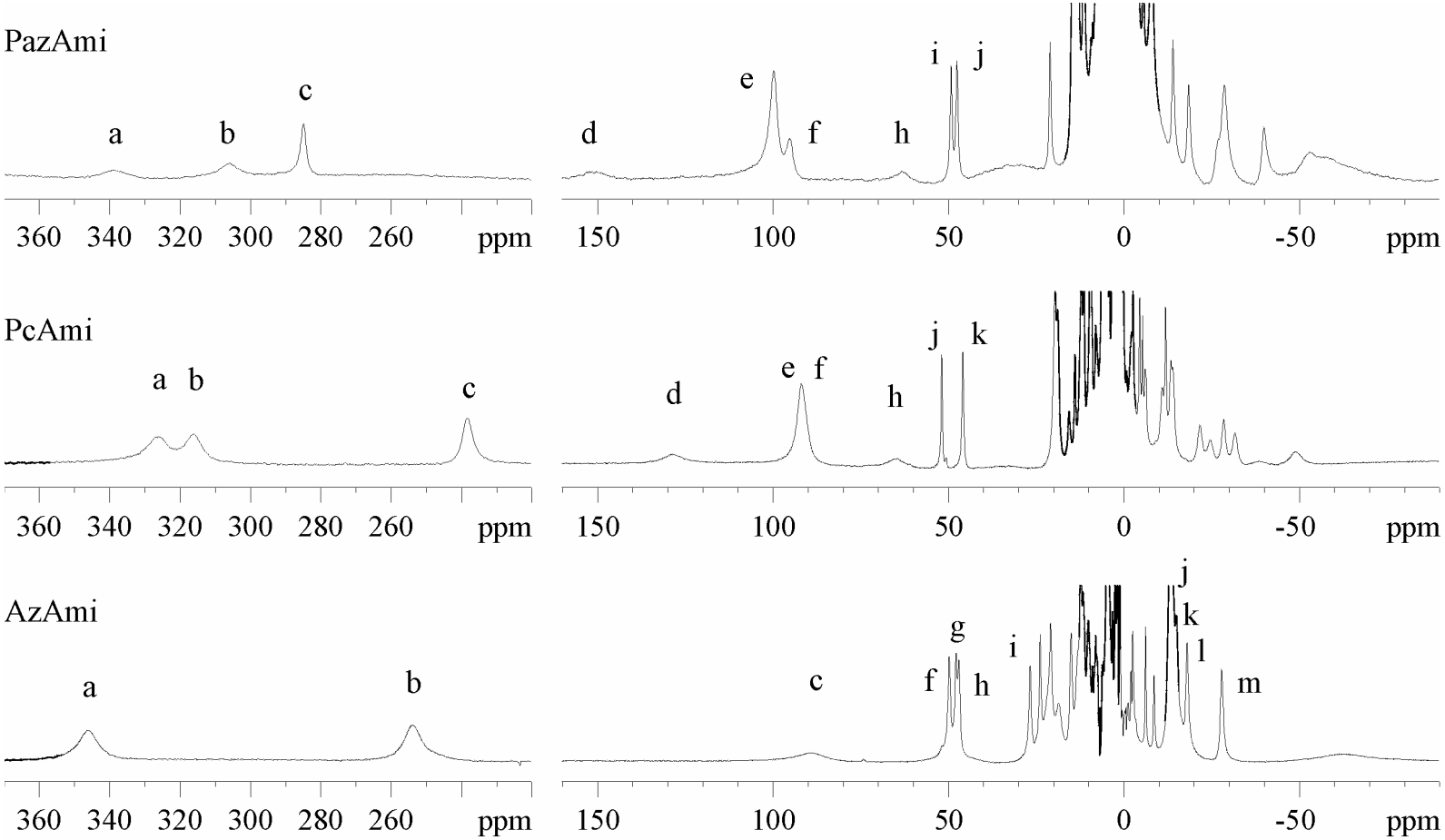

Figure S6. ^{1}H NMR spectra (300 MHz) of the Co(II) loop contraction variants (25 $^{\circ}$C) in 99.9 % deuterated 10 mM phosphate buffer at pH* 8.1.

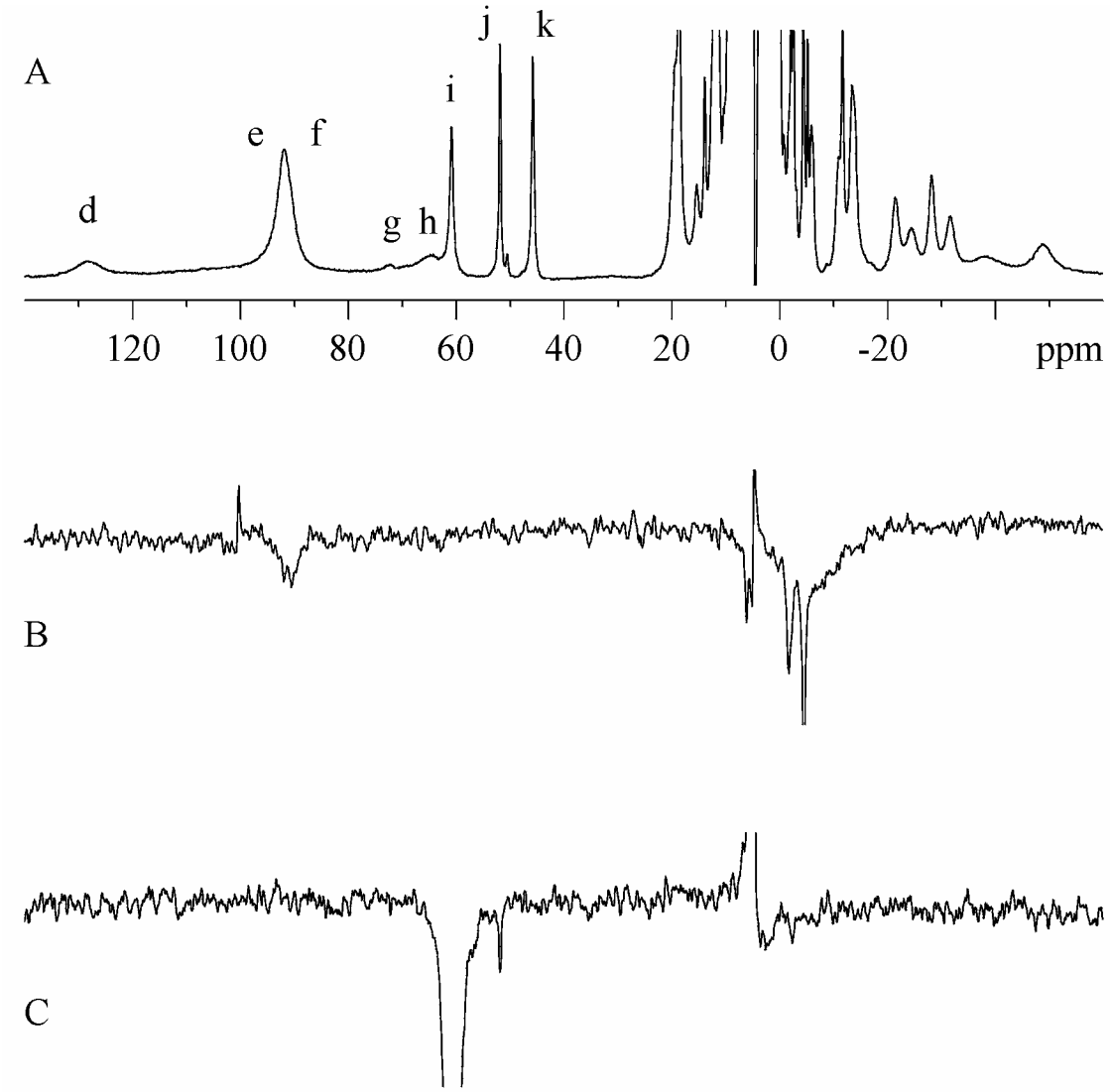

Figure S7. ^{1}H NMR spectrum (A) of Co(II) PcAmi (25 °C) in 10 mM phosphate (90 % H_2O / 10 % D_2O) at pH 8.1. Also shown are 1D NOE difference experiments (B and C) in which peaks c and i were irradiated.

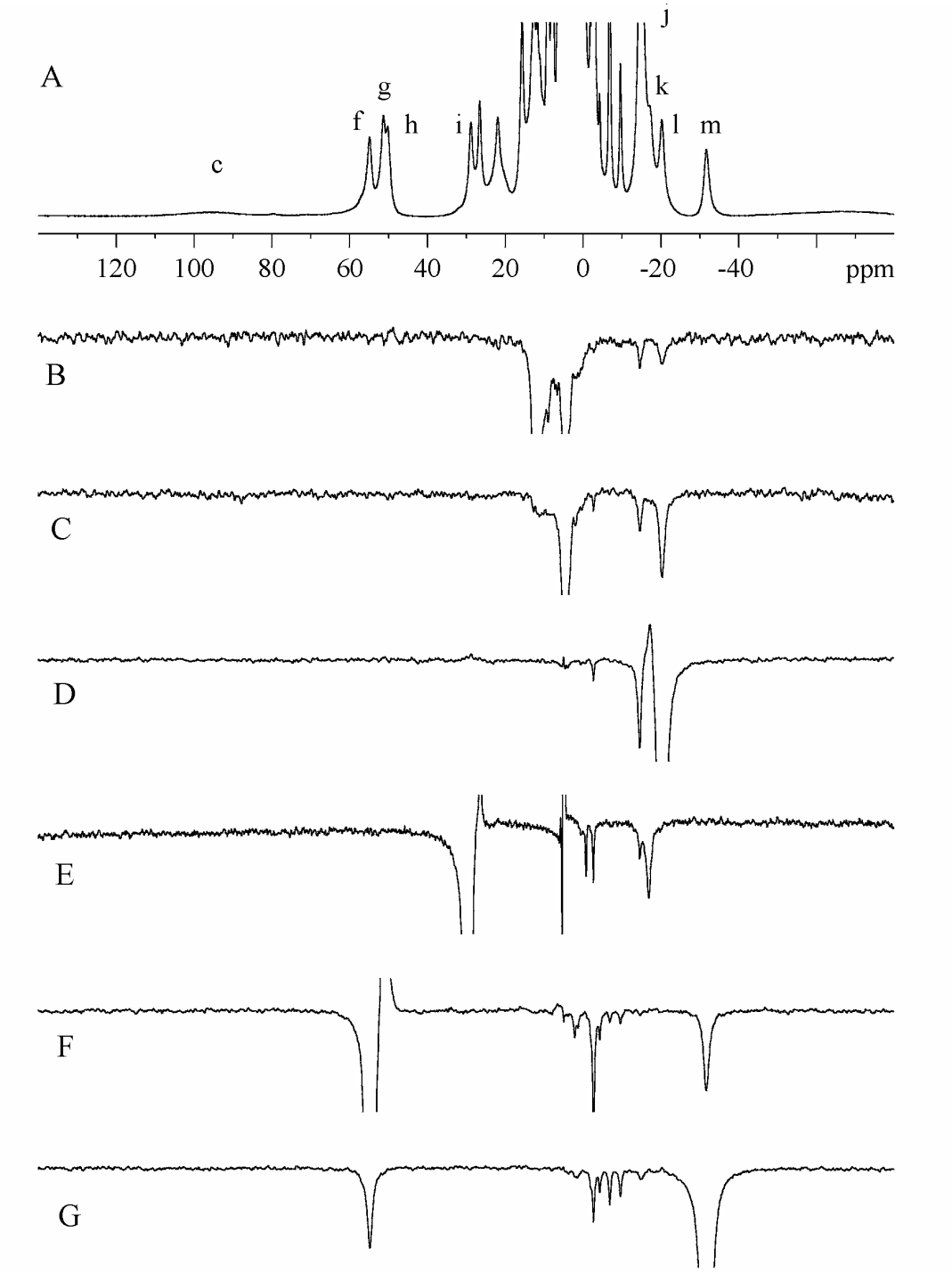

Figure S8. ^{1}H NMR spectrum (A) of Co(II) AzAmi (5 °C) in 10 mM phosphate (99.9 % D_2O) at pH* 8.1. Also shown are 1D NOE difference experiments (B-G) in which peaks a, b, l, i, f and m respectively were irradiated.

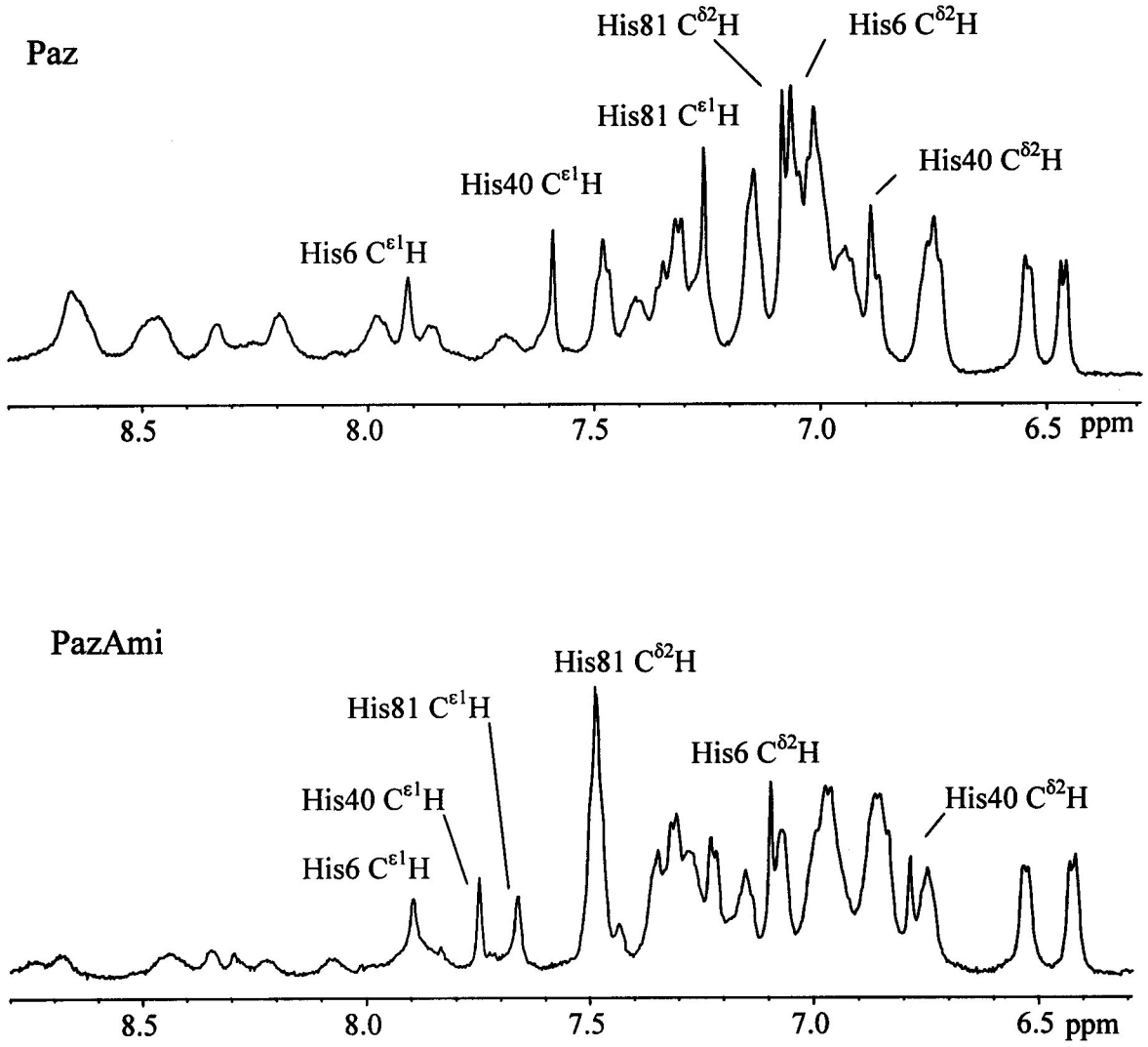

Figure S9. Part of the aromatic region of the ^{1}H NMR spectra (500 MHz) of Cu(I) Paz (pH* 7.6) and PazAmi (pH* 7.5) in 10 mM phosphate (99.9 % D_2O) at 25 °C.

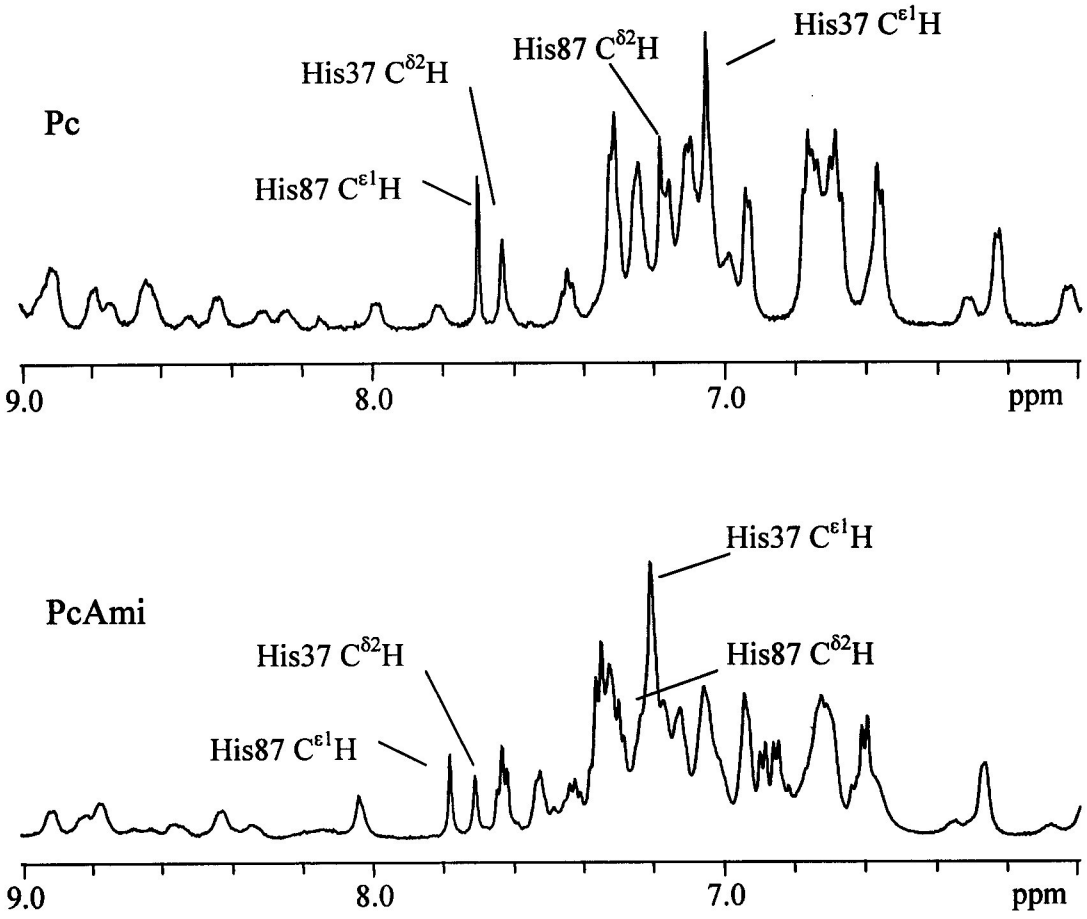

Figure S10. Part of the aromatic region of the ^{1}H NMR spectra (500 MHz) of Cu(I) Pc (pH* 7.5) and PcAmi (pH* 7.6) in 100 mM phosphate (99.9 % D_2O) at 25 °C.

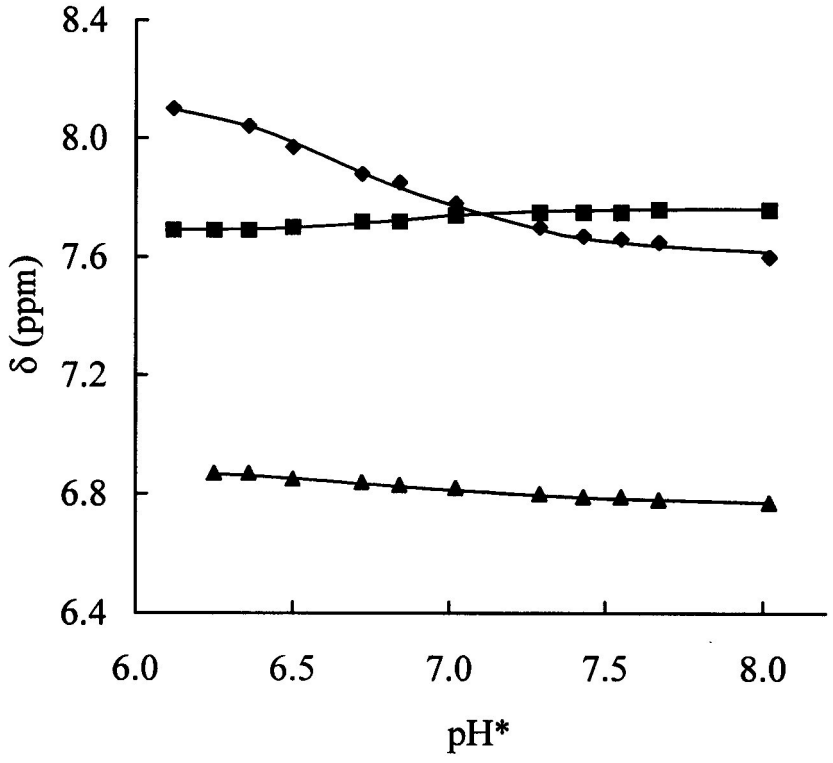

Figure S11. Dependence on pH* of the chemical shift of the His81 $C^{\varepsilon 1}H$ (◆), His40 $C^{\varepsilon 1}H$ (■) and His40 $C^{\delta 2}H$ (▲) resonances in the ^1H NMR spectrum of PazAmi in 10 mM phosphate (25 °C). The solid lines are the fits of the data and result in pK_a* values of 6.7, 6.7 and 6.8 respectively.

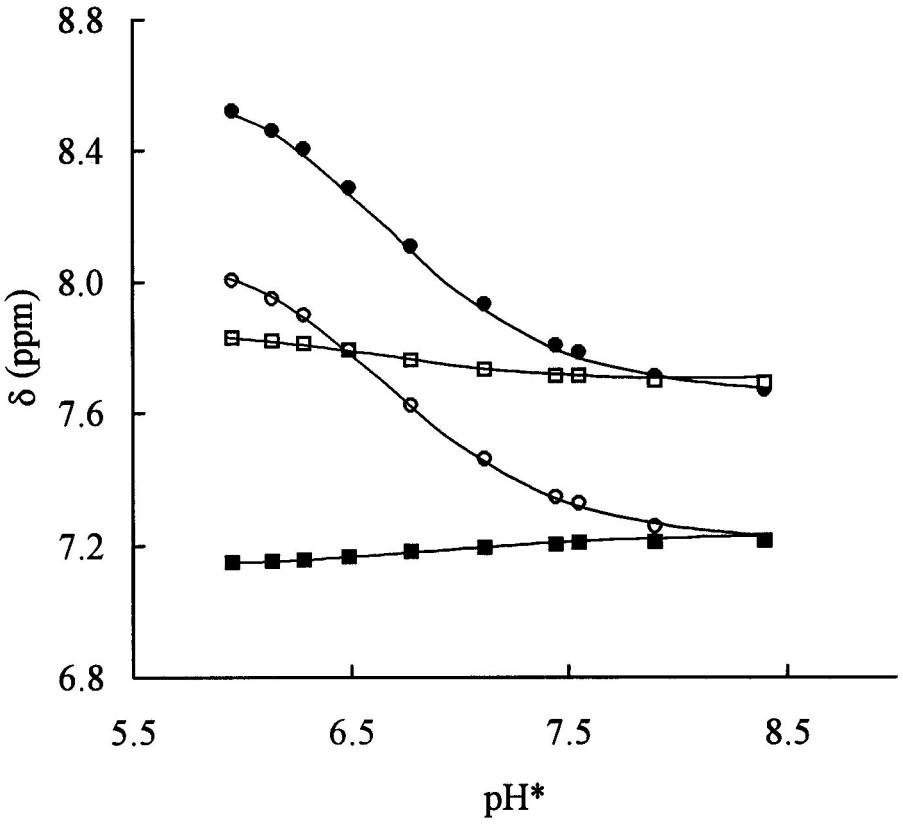

Figure S12. Dependence on pH* of the chemical shift of the His87 $C^{\varepsilon 1}H$ (•), His87 $C^{\delta 2}H$ (o), His37 $C^{\delta 2}H$ (□) and His37 $C^{\varepsilon 1}H$ (■) resonances in the ^1H NMR spectrum of PcAmi in 100 mM phosphate (25 °C). The solid lines are the fits of the data and result in pK_a* values of 6.7 for all resonances.

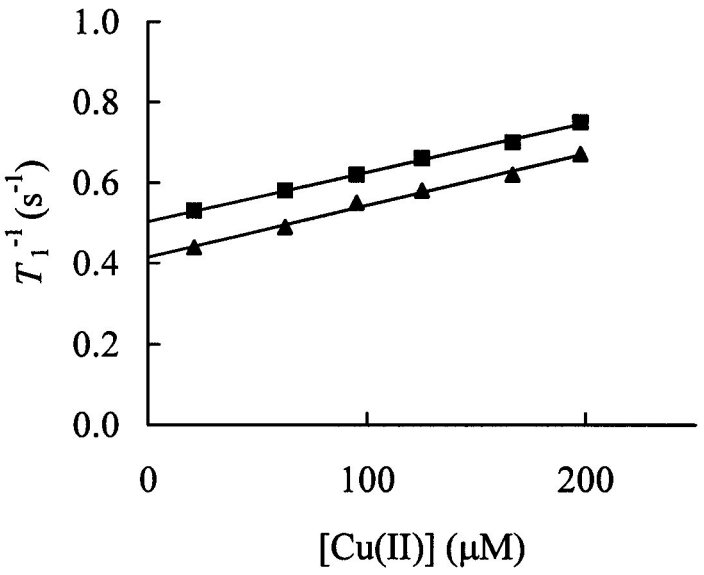

Figure S13. Plots (25 °C) of T_1^{-1} against [Cu(II)] for the His87 $C^{\varepsilon 1}H$ (▲) and His37 $C^{\delta 2}H$ (■) resonances of PcAmi in 37 mM phosphate buffer (99.9 % D_2O) at pH* 7.5 (I = 0.10 M). The error bars are smaller than the symbols.

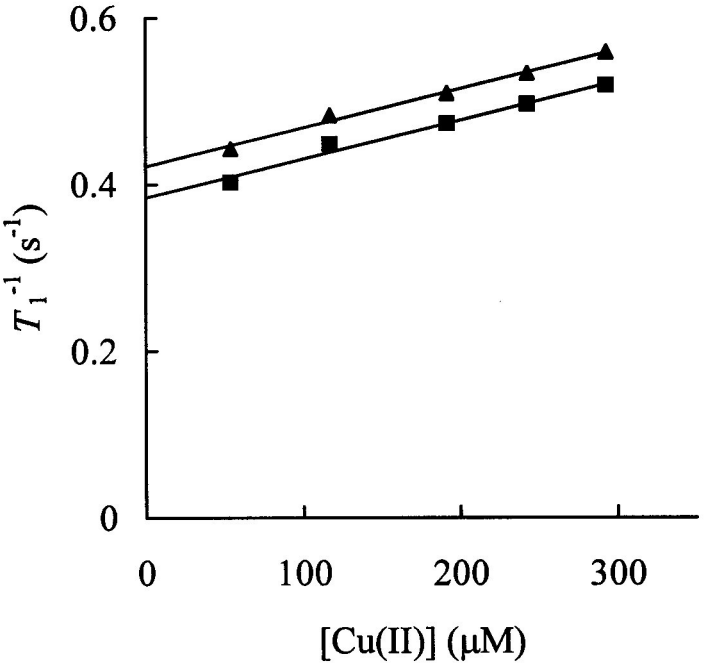

Figure S14. Plots (25 °C) of T_1^{-1} against [Cu(II)] for the His40 $C^{\delta 2}H$ (▲) and His81 $C^{\varepsilon 1}H$ (■) resonances of PazAmi in 37 mM phosphate (99.9 % D_2O) at pH* 7.6 (I = 0.10 M). The error bars are smaller than the symbols.

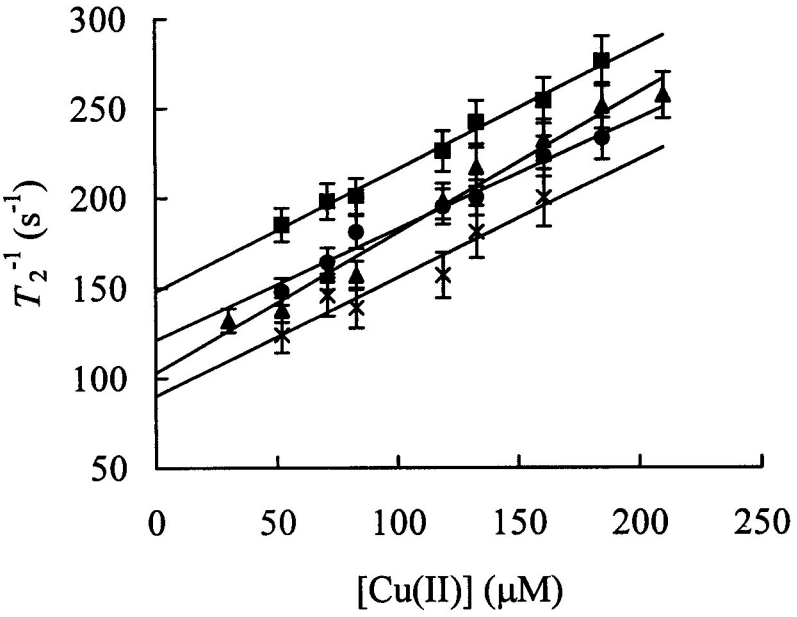

Figure S15. Plots (25 °C) of T_2^{-1} against [Cu(II)] for the Met118 $C^{\varepsilon}H_3$ (■), His46 $C^{\beta}H$ (•) and the Cys112 $C^{\alpha}H$ (▲) resonances plus the signal at 6.1 ppm (x) in the spectrum of WEFT spectrum of AzAmi in 20 mM phosphate (99.9 % D_2O) at pH* 8.2.